Zero refractive index materials and topological photonics

S. A. R. Horsley[1], M. Woolley[2]

[1]*Department of Physics and Astronomy,*

University of Exeter, Stocker Road, Exeter EX4 4QL

[2]*School of Natural Sciences,*

University of Exeter, North Park Road, Exeter EX4 4QF

(Dated: August 19, 2020)

Abstract

The refractive index is one of the most basic optical properties of materials and their interaction with light. Modern materials engineering—particularly the concept of metmaterials—has made it necessary to consider its subtleties, including anisotropy and complex values. Here, we re–examine the refractive index and find a general way to calculate the direction-dependent refractive index, and the condition for zero index in a given direction. By analogy with linear versus circular polarization, we show that when the zero–index direction is complex valued the material supports waves that can propagate in only one sense, e.g. clockwise. We show that there are an infinite family of both time-reversible and time-irreversible homogeneous electromagnetic media that support unidirectional propagation for a particular polarization. As well as extending the concept of the refractive index, shedding new light on our understanding of topological photonics, and giving new sets of material parameters, our simple picture also reproduces many of the findings derived using topology.

INTRODUCTION

A ray of light changes direction when passing from one material into another; it refracts. Formulated by Persian physicist Ibn Sahl [1], this was one of the first effects to be captured in a mathematical law. Yet the index of refraction n wasn't introduced until nearly a thousand years later [2]. Maxwell's theory has since made it clear that the refractive index relates the wavelength in free space to that in the material, and—in an isotropic material—is equal to the square root of the product of permittivity and permeability, $n = \sqrt{\epsilon\mu}$.

Due to a growth in available materials [3], the concept of refractive index is more subtle in modern physics. Materials are generally anisotropic, meaning that the refractive index depends on both polarization and direction of propagation. The index can also be complex valued, an imaginary part indicating the degree to which the material absorbs or amplifies the wave, leading to counter intuitive wave effects that are still the subject of active research [4, 5]. Its real part can also be either positive or negative, with a negative refractive index giving a reversal of the phase velocity, bending the wave in a direction that is impossible with positive index media [6]. The refractive index can also take values very close to zero [7], where the wavelength becomes arbitrarily large and distant points are electromagnetically close, as in Maxwell's Fish Eye lens [8]. Near perfect transmission of electromagnetic waves can be achieved through small zero index channels [9], and unusual boundary conditions can be realised, such as those of an effective magnetic conductor [10].

Near zero index materials are the subject of this work. The motivation is recent work on one–way propagation in homogeneous gyrotropic media [11–14]. Media exhibiting one–way propagation are typically designed using the mathematics of topology, and involve rather cumbersome calculations. It is simpler to calculate a zero in the refractive index than to calculate a Chern number. We develop an understanding of zeros in the refractive index that can be applied to design materials that support unidirectional propagation. We find a general condition for such media, predicting new wave effects, and reproducing many of the existing findings in the topological photonics literature.

ZERO INDEX MATERIALS AND TOPOLOGICAL INSULATORS

We start with an observation concerning the 2D Dirac equation for a particle of mass m and energy $\hbar\omega$ [15]: the canonical model of a topological insulator [16].

$$\left(-\mathrm{i}\boldsymbol{\sigma}\cdot\boldsymbol{\nabla}+\frac{mc}{\hbar}\sigma_z-\frac{\omega}{c}\right)|\psi\rangle=\begin{pmatrix}\frac{mc}{\hbar}-\frac{\omega}{c} & -\mathrm{i}\left(\frac{\partial}{\partial x}-\mathrm{i}\frac{\partial}{\partial y}\right)\\ -\mathrm{i}\left(\frac{\partial}{\partial x}+\mathrm{i}\frac{\partial}{\partial y}\right) & -\frac{mc}{\hbar}-\frac{\omega}{c}\end{pmatrix}\begin{pmatrix}\psi_a\\ \psi_b\end{pmatrix}=0 \qquad (1)$$

where $\boldsymbol{\sigma}=\sigma_x\hat{\boldsymbol{x}}+\sigma_y\hat{\boldsymbol{y}}$. This equation is an expression of the relativistic dispersion relation, and is an approximate description of e.g. the lowest two bands of propagation in a honeycomb lattice. For energies of greater magnitude than the rest energy $\hbar|\omega|>mc^2$, the solutions are propagating and the wave vector is real. For smaller magnitude energies, they are exponentially decaying.

At the transition point between this aforementioned conducting and insulating behaviour, the square of the wave vector vanishes. This is equivalent to a zero in the refractive index. However, it is an unusual form of zero index condition. For instance, the out of plane electric field E_z of a monochromatic wave in an isotropic material obeys the Helmholtz equation, which in the zero index limit becomes Laplace's equation

$$\boldsymbol{\nabla}^2E_z=4\frac{\partial^2E_z}{\partial\mathcal{Z}\partial\mathcal{Z}^\star}=0 \qquad (2)$$

where $\mathcal{Z}=x+\mathrm{i}y$. The solutions are analytic functions of *either* $\mathcal{Z}$ or $\mathcal{Z}^\star$. Yet in the case of the 2D Dirac equation (1) when $\hbar\omega=mc^2$, the second component of the wavefunction satisfies

$$2\frac{\partial\psi_b}{\partial\mathcal{Z}}=0. \qquad (3)$$

Equation (3) is equivalent to the Cauchy–Riemann equations for an analytic function of $\mathcal{Z}^\star$. In a sense this is half of the Laplace equation (2). Waves obeying the Cauchy–Riemann equations propagate in only one sense around the origin. Writing the Taylor expansion of the solution to equation (3) in polar coordinates $\mathcal{Z}=r\,\mathrm{e}^{\mathrm{i}\theta}$

$$\psi_b=\sum_{n=0}^{\infty}c_n\,r^n\,\mathrm{e}^{-\mathrm{i}n\theta} \qquad (4)$$

we observe the series contains only clockwise propagating waves. This one–way propagation is indicative of the transition of the Dirac equation (1) from conducting to the (topological) insulating state. Further details are given in the supplementary material. In this work we will find electromagnetic materials within which the field has the same properties.

THE 6–VECTOR FORM OF MAXWELL'S EQUATIONS

A general linear electromagnetic material can be characterised in terms of its constitutive relations, relating the displacement field $\boldsymbol{D}$ and magnetic flux density $\boldsymbol{B}$ to the electric field $\boldsymbol{E}$ and magnetizing field $\boldsymbol{H}$. The most general local constitutive relations for *lossless* media take the form

$$\begin{aligned} \boldsymbol{D} &= \epsilon_0 \boldsymbol{\epsilon} \cdot \boldsymbol{E} + \frac{1}{c} \boldsymbol{\xi} \cdot \boldsymbol{H} \\ \boldsymbol{B} &= \mu_0 \boldsymbol{\mu} \cdot \boldsymbol{H} + \frac{1}{c} \boldsymbol{\xi}^\dagger \cdot \boldsymbol{E}. \end{aligned} \tag{5}$$

where $\boldsymbol{\epsilon}$ and $\boldsymbol{\mu}$ are Hermitian tensors and $\boldsymbol{\xi}$ is an arbitrary complex tensor. For simplicity we restrict ourselves to the lossless case. When $\boldsymbol{\epsilon}$, $\boldsymbol{\mu}$, and $\boldsymbol{\xi}$ are all non–zero, the medium is known as bianisotropic. Examples of such materials include moving dielectrics; collections of small chiral inclusions; and arrays of split ring resonators.

We now find the propagation characteristics of waves in such media. Given that material parameters are generally a function of frequency, we take fields of a fixed frequency ω, and write Maxwell's equations compactly in terms of a single 6–vector $F = (\boldsymbol{E}, \eta_0 \boldsymbol{H})^{\mathrm{T}}$

$$\mathcal{D} F = k_0 \chi F \tag{6}$$

where $\eta_0 = \sqrt{\mu_0/\epsilon_0}$ is the free space impedance, and $\mathcal{D}$ and χ are the Hermitian operators

$$\mathcal{D} = \begin{pmatrix} \mathbf{0} & \mathrm{i}\boldsymbol{\nabla}\times \\ -\mathrm{i}\boldsymbol{\nabla}\times & \mathbf{0} \end{pmatrix}, \qquad \chi = \begin{pmatrix} \boldsymbol{\epsilon} & \boldsymbol{\xi} \\ \boldsymbol{\xi}^\dagger & \boldsymbol{\mu} \end{pmatrix}. \tag{7}$$

As discussed in [14, 17–19], equation (6) has a great deal in common with the Dirac equation.

In an infinite homogeneous medium, the field vector F can be assumed to have an $\exp(\mathrm{i}k\boldsymbol{n}\cdot\boldsymbol{x})$ dependence, where the wave vector $\boldsymbol{k} = k\boldsymbol{n}$ has magnitude $|k|$ and direction $\boldsymbol{n}$. In general the magnitude of the wave–vector (i.e. the refractive index) will depend on the direction of propagation. Substituting this form of the field in equation (6), the ratio k_0/k can be calculated as an eigenvalue problem

$$\chi^{-1} \begin{pmatrix} \mathbf{0} & -\boldsymbol{n}\times \\ \boldsymbol{n}\times & \mathbf{0} \end{pmatrix} F = \frac{k_0}{k} F \tag{8}$$

The 6×6 matrix on the left of equation (8) has six eigenvalues k_0/k_m and eigenvectors F_m. Given that both matrices on the left of (8) are Hermitian, the eigenvectors F_n are orthogonal

with respect to the inner product,

$$F_n^\dagger \chi F_m = \pm\delta_{nm} \qquad (n \neq m) \tag{9}$$

where the eigenvalues k_m are assumed real, and the sign of the right hand side of (9) is not necessarily positive because e.g. χ could be negative definite. Two of the eigenvalues of equation (8) are zero, corresponding to the static fields with the longitudinal eigenvectors $(\boldsymbol{n}, \boldsymbol{0})^{\mathrm{T}}$ and $(\boldsymbol{0}, \boldsymbol{n})^{\mathrm{T}}$. The remaining four eigenvalues come in two pairs of equal magnitude and opposite sign: the two electromagnetic polarizations, propagating in either direction.

The magnitude of the refractive index for each of the modes is given by the magnitude of the inverse of the eigenvalues k_0/k_m. The sign of the index is determined by whether the time averaged Poynting vector $\boldsymbol{S} = \mathrm{Re}[\boldsymbol{E} \times \boldsymbol{H}^\star]/2$ is parallel or anti–parallel to the wave–vector $\boldsymbol{k} = k_m \boldsymbol{n}$, i.e. it is the sign of $\boldsymbol{k} \cdot \boldsymbol{S}$

$$\begin{aligned} \mathrm{sign}\left[\boldsymbol{k} \cdot \boldsymbol{S}\right] &= \mathrm{sign}\left[k_m \boldsymbol{n} \cdot \frac{1}{2}\mathrm{Re}\left[\boldsymbol{E} \times \boldsymbol{H}^\star\right]\right] = \mathrm{sign}\left[k_m F_m^\dagger \, N(\boldsymbol{n}) \, F_m\right] \\ &= \mathrm{sign}\left[F_m^\dagger \chi F_m\right] \end{aligned} \tag{10}$$

where we applied equation (8). The sign of the refractive index for the eigenmode F_m is thus determined by the sign of the inner product $F_m^\dagger \, \chi \, F_m$. Media where every mode propagates with a negative index are thus characterized as having a negative definite material tensor χ.

REAL AND COMPLEX AXIS ZERO INDEX MEDIA

Zero index media are those where one or more of the eigenvalues of the material tensor χ are zero. To see this, assume propagation in the x–y plane, where the field is determined by the out of plane electric E_z and magnetic H_z fields. We take the inner product of Maxwell's equations (6) with the normalized vector $V = \mathrm{i}(\cos(\psi)\boldsymbol{m} \times \hat{\boldsymbol{z}}, -\sin(\psi)\mathrm{e}^{\mathrm{i}\sigma}\boldsymbol{m} \times \hat{\boldsymbol{z}})^{\mathrm{T}}$

$$V^\dagger \mathcal{D} F = \boldsymbol{m} \cdot \boldsymbol{\nabla}\Psi = k_0 \, V^\dagger \chi F. \tag{11}$$

The left hand side of (11) is the gradient of the combination of out of plane fields, $\Psi = \sin(\psi)\mathrm{e}^{-\mathrm{i}\sigma}E_z + \cos(\psi)\eta_0 H_z$, along the $\boldsymbol{m} = m_x\hat{\boldsymbol{x}} + m_y\hat{\boldsymbol{y}}$ axis (choices of V where $\boldsymbol{m}$ points out of the plane correspond to a coupling between in–plane and out–of plane fields which we do not analyse here).

If the index is zero in the $\boldsymbol{m}$ direction for the combination of fields Ψ, the right hand side of (11) is zero. We can ensure this if V is a zero eigenvector of the constitutive tensor χ,

$$V^\dagger \chi = 0. \tag{12}$$

A zero in the refractive index is therefore associated with a zero eigenvalue of the material tensor χ. The refractive index in the $\boldsymbol{m}$ direction can be parameterized through introducing the projection $P = 1_6 - \lambda V \otimes V^\dagger$ (λ real, between 0 and 1), using it to define a new tensor

$$\chi = P\,\chi_{\rm i}\,P \tag{13}$$

which equals the initial material tensor $\chi_{\rm i}$ when $\lambda = 0$, and has zero index in the $\boldsymbol{m}$ direction when $\lambda = 1$.

FIG. 1. Dispersion relation (lower panels) and polarization (upper panels) for electromagnetic waves in materials as the index is reduced to zero. (a) Dispersion and polarization in a material with parameters $\boldsymbol{\epsilon} = 21_3$, $\boldsymbol{\mu} = 1_3$ and $\boldsymbol{\xi} = 0$. (b) Dispersion and polarization for the projected material tensor χ from equation (13), for zero index in a direction at 23 degrees to the x–axis (black dashed line). Parameters are $\psi = 0$; $\sigma = \pi/2$ (here arbitrary); and $\boldsymbol{m} = 0.911\,\hat{\boldsymbol{x}} + 0.397\,\hat{\boldsymbol{y}}$. (c–d) Material approaching zero index in the arbitrarily chosen *complex* direction, $\boldsymbol{m} = (0.656 - 0.286\mathrm{i})\hat{\boldsymbol{x}} + (0.296 + 0.633\mathrm{i})\hat{\boldsymbol{y}}$. The remaining parameters are $\psi = 3\pi/10$ and $\sigma = \pi/2$. (c) Initial material ($\lambda = 0$) is that in (a–b), and in (d) it is a randomly generated lossless material (see the supplementary material). Note that panel (d) shows the polarization of the zero index mode may depend on the angle of propagation.

Figure 1 shows a numerical example, taking an isotropic dielectric and projecting out a real space direction and polarization according to (13). As λ approaches 1, this results in an increasingly anisotropic material, squashing the dispersion circle into an infinitely thin ellipse. In the supplementary material we demonstrate agreement with a full wave simulation, and for an initial material generated using a random number generator.

This characterization of zero index media connects to the earlier discussion of the Dirac equation. Suppose the zero index direction $\boldsymbol{m}$ in (11) is complex valued: for example $\boldsymbol{m} = (\hat{\boldsymbol{x}} + \mathrm{i}\hat{\boldsymbol{y}})/\sqrt{2}$. This special case was recently associated with uni–directional wave propagation and photonic edge states in gyrotropic media [13]. For this form of $\boldsymbol{m}$, equation

FIG. 2. Emission from a circulating current inside a CAN medium. (a–c) Emission from a circulating current (panel (a), $\boldsymbol{e}_d = \hat{\boldsymbol{x}} + \mathrm{i}\hat{\boldsymbol{y}}$, panel (b) $\boldsymbol{e}_d = \hat{\boldsymbol{x}} - \mathrm{i}\hat{\boldsymbol{y}}$) in a homogeneous material. Here $a = 1$, and the saturation of the image indicates the magnitude of the field (panels (a) and (b) are on the same scale). (c) The emitted power relative to free space, with the crosses the result of the simulation, and the solid line given by equation (17). (d–f) Same as (a–c), but the CAN medium is a cylinder of 5 wavelengths radius, surrounded by free space.

(11) becomes

$$\left(\frac{\partial}{\partial x} + \mathrm{i}\frac{\partial}{\partial y}\right)\Psi = 2\frac{\partial \Psi}{\partial \mathcal{Z}^\star} = 0. \tag{14}$$

As in the case of the two dimensional Dirac equation this is equivalent to the Cauchy–Riemann conditions. This has a rather different interpretation to the previous case where $\boldsymbol{m}$ was real. Instead of squashing the dispersion circle into a thin ellipse, it closes to a point as shown in figure 1c–d. This is because the zero index condition is $(\boldsymbol{m}' + \mathrm{i}\boldsymbol{m}'')\cdot\boldsymbol{k} = 0$ which—unless $\boldsymbol{m}'$ and $\boldsymbol{m}''$ are parallel—implies $\boldsymbol{k} = 0$, for real $\boldsymbol{k}$. When the zero index condition is satisfied, the out of plane field is allowed to propagate in only one sense around the origin. For brevity we'll refer to these materials as complex axis nihility (CAN) media. The one–way propagation is evident if we write the Taylor expansion of Ψ in polar coordinates (as in equation (4)): the series contains only positive powers of the complex coordinate $\mathcal{Z}$, a restriction that comes from demanding no singularities in the field, and requires the medium to be simply connected.

EXAMPLES

Circulation dependent density of states in a CAN medium

The power emitted by a source in a CAN medium is very sensitive to the sense of rotation of the current. To demonstrate this dependence we take H polarized radiation generated by an in–plane current, surrounded by a gyrotropic material with out of plane permeability μ_{zz} and in plane permittivity

$$\boldsymbol{\epsilon} = \begin{pmatrix} a & -\mathrm{i}b \\ \mathrm{i}b & a \end{pmatrix} = a1_3 + \mathrm{i}b\hat{\boldsymbol{z}}\times . \tag{15}$$

In the limit $a \to \pm b$ this medium has zero index in the complex direction $\hat{\boldsymbol{x}} \pm \mathrm{i}\hat{\boldsymbol{y}}$, as can be verified from equation (12). The source extends along the z–axis, and has an in–plane current density $\boldsymbol{j}(\boldsymbol{x}) = j_0 \boldsymbol{e}_d \delta^{(2)}(\boldsymbol{x} - \boldsymbol{x}_0)$, where $\boldsymbol{e}_d$ is the direction of current flow. For this form of current, the cycle averaged emitted power is given by

$$\langle P_{\boldsymbol{e}_d} \rangle = \frac{k_0 \eta_0 \mu_{zz} |j_0|^2}{2} \mathrm{Im}[\boldsymbol{e}_d^\star \cdot \boldsymbol{G}(\boldsymbol{x}_0, \boldsymbol{x}_0) \cdot \boldsymbol{e}_d] \tag{16}$$

where $\mathrm{Im}[\boldsymbol{e}_d^\star \cdot \boldsymbol{G}(\boldsymbol{x}_0, \boldsymbol{x}_0) \cdot \boldsymbol{e}_d]$ is proportional to the partial local density of states [20], with $\boldsymbol{G}$ the dyadic Green function. The supplementary material gives the defining differential equation, and the calculation of this Green function. Now consider two circulations of the current, with cycle averaged power $\langle P_{\circlearrowleft} \rangle$ for $\boldsymbol{e}_d = (\hat{\boldsymbol{x}} + \mathrm{i}\hat{\boldsymbol{y}})/\sqrt{2}$, and $\langle P_{\circlearrowright} \rangle$ for $\boldsymbol{e}_d = (\hat{\boldsymbol{x}} - \mathrm{i}\hat{\boldsymbol{y}})/\sqrt{2}$. Evaluating (16) for these two unit vectors gives

$$\begin{aligned} \langle P_{\circlearrowleft} \rangle &= \frac{\eta_0 \mu_{zz} k_0 |j_0|^2}{16 a^2} (a - b)^2 \\ \langle P_{\circlearrowright} \rangle &= \frac{\eta_0 \mu_{zz} k_0 |j_0|^2}{16 a^2} (a + b)^2. \end{aligned} \tag{17}$$

Therefore when the material (15) satisfies our zero index condition (12) for the complex propagation direction $\hat{\boldsymbol{x}} \pm \mathrm{i}\hat{\boldsymbol{y}}$ ($a \to \pm b$), the density of states vanishes for one of the two senses of current circulation. This means that—as shown in equation (17)—very little power can be emitted for current of one sense of circulation versus the other. Figure 2 shows the results of a full wave simulation, verifying equation (17), and also demonstrating the same asymmetry in emission for a cylinder of CAN material.

Scattering from a CAN cylinder

These materials also scatter waves in a manner that is sensitive to their angular momentum, excluding one sense of circulation from the material. To demonstrate this we work in the polarization basis $\Psi = E_z + \eta_0 H_z$, taking the zero index direction as $\boldsymbol{m} = \hat{\boldsymbol{x}} + \mathrm{i}\hat{\boldsymbol{y}}$. Expanding out our zero index condition (11) in this polarization basis we have

$$2 \frac{\partial}{\partial \mathcal{Z}^\star} (E_z + \eta_0 H_z) = k_0 \left[\boldsymbol{m} \cdot (\boldsymbol{\epsilon} - \boldsymbol{\xi}^\dagger) \cdot \boldsymbol{E} - \boldsymbol{m} \cdot (\boldsymbol{\mu} - \boldsymbol{\xi}) \cdot \eta_0 \boldsymbol{H} \right] = 0 \tag{18}$$

which shows that the CAN medium satisfies

$$\boldsymbol{m} \cdot \left(\boldsymbol{\epsilon} - \boldsymbol{\xi}^\dagger \right) = 0, \qquad \boldsymbol{m} \cdot (\boldsymbol{\mu} - \boldsymbol{\xi}) = 0. \tag{19}$$

One of the many possible ways to fulfill these conditions is to choose the permittivity and permeability as isotropic (in this case equal to the unit tensor), and the bianisotropy as imaginary and antisymmetric

$$\boldsymbol{\epsilon} = 1_3,\ \boldsymbol{\mu} = 1_3,\ \boldsymbol{\xi} = \lambda \begin{pmatrix} 0 & \mathrm{i} & 0 \\ -\mathrm{i} & 0 & 0 \\ 0 & 0 & 0 \end{pmatrix}. \tag{20}$$

In the limit $|\lambda| \to 1$ this material satisfies the zero index condition (19). Unlike the gyrotropic material of the previous example, this material is time reversible: taking $\boldsymbol{H} \to -\boldsymbol{H}$ and $\mathrm{i} \to -\mathrm{i}$ leaves the constitutive relations (5) unchanged. This bianisotropic response given in (20) can be obtained from an array of small Omega shaped wire particles [21, 22] (although here $\boldsymbol{\epsilon} = \boldsymbol{\mu}$). At first sight time reversibility seems at odds with a sensitivity to the sense of wave circulation. But we achieve this in the same manner as [23]: the time irreversiblity comes from the polarization basis, which upon time reversal undergoes the transformation $E_z + \eta_0 H_z \to E_z - \eta_0 H_z$. Silveirinha's recent work [21] includes an interesting discussion of scattering anomalies in media with these constitutive relations.

FIG. 3. Scattering from a bianisotropic CAN medium. The material parameters are given in equation (20), with $\lambda = 0.999$. The radius of cylinder is $k_0 R = 7.54$, and $r_{l,0}$ refers to the partial wave scattering amplitude obtained when the wave satisfies $\Psi = 0$ on the surface of the cylinder. (a–b) Magnitude and phase of the reflected partial wave amplitudes $r_{l,+}$ which are equal to $r_{l,0}$ for $l < 0$. (c–d) Partial sums of the angular momentum field components, over the indicated range of angular momenta. Panel (d) shows that negative angular momentum are completely excluded from the cylinder.

Take a plane wave incident onto a cylinder of radius R composed of the bianisotropic material defined in (20). Within the cylinder, Maxwell's equations can be written as the pair; $\boldsymbol{\nabla}\Psi \times \hat{\boldsymbol{z}} = \mathrm{i}k_0 \left(1_2 + \mathrm{i}\lambda \hat{\boldsymbol{z}}\times\right) \cdot \boldsymbol{\Phi}$, and $\boldsymbol{\nabla} \times \boldsymbol{\Phi} = -\mathrm{i}k_0 \Psi$, where $\boldsymbol{\Phi} = \eta_0 \boldsymbol{H}_{\|} - \boldsymbol{E}_{\|}$, with '$\|$' indicating field components in the plane of propagation. Eliminating the in–plane field $\boldsymbol{\Phi}$ yields

$$\boldsymbol{\nabla}^2 \Psi + k^2 \Psi = 0 \tag{21}$$

where $k^2 = (1 - \lambda^2) k_0^2$. This is simply the Helmholtz equation for a scalar wave in a medium with refractive index $n = \sqrt{1 - \lambda^2}$. We use the generating function for Bessel functions [24]

to represent the incident wave as the sum $\exp(\mathrm{i}k_0 x) = \sum_l \mathrm{i}^l J_l(k_0 r)\exp(\mathrm{i}l\theta)$, and outside the cylinder the total field therefore takes the form

$$\Psi(r,\theta) = \sum_{l=-\infty}^{\infty} \mathrm{i}^l \left[J_l(k_0 r) + r_l \mathcal{H}_l^{(0)}(k_0 r)\right] \mathrm{e}^{\mathrm{i}l\theta} \qquad r > R \tag{22}$$

where J_n and $\mathcal{H}_n^{(0)}$ are Bessel and Hankel functions of the first kind, respectively. Expanding Ψ within the cylinder as a series of Bessel functions of the first kind and enforcing the continuity of the tangential electric and magnetic fields yields the partial wave reflection coefficient (for further details see supplementary material)

$$r_l = -\frac{J_l'(k_0 R) - \mathrm{i}\frac{Z_l}{\eta_0} J_l(k_0 R)}{\mathcal{H}_l'^{(0)}(k_0 R) - \mathrm{i}\frac{Z_l}{\eta_0}\mathcal{H}_l^{(0)}(k_0 R)} \tag{23}$$

where the quantity Z_l is analogous to the surface impedance and here takes the form

$$Z_l = -\frac{\mathrm{i}\eta_0}{1-\lambda^2}\left(\frac{k}{k_0}\frac{J_l'(kR)}{J_l(kR)} - \frac{l\lambda}{k_0 R}\right) \sim -\frac{\mathrm{i}\eta_0|l|}{k_0 R}\lim_{\lambda\to+1}\frac{(1-\mathrm{sign}[l]\lambda)}{(1-\lambda)(1+\lambda)}. \tag{24}$$

The approximation on the right of (24) comes from taking the zero index limit $\lambda \to +1$. The electrical radius kR becomes small so that $J_l'(kR)/J_l(kR) \sim |l|/kR$ [24]. For negative angular momenta $l < 0$, Z_l diverges, whereas for positive angular momenta $l > 0$, Z_l does not diverge, taking the form $Z_l = -\mathrm{i}\eta_0|l|/2k_0 R$. A divergent Z_l leads to a partial wave reflection coefficient $r_l = -J_l(k_0 R)/\mathcal{H}_l^{(0)}(k_0 R)$ which—as can be seen from equation (22)—is the same as for a cylinder where $\Psi = 0$ on the surface. Therefore the partial waves with negative angular momentum are set to zero on the surface of the CAN cylinder, in agreement with the expectation that Ψ should become an analytic function of $\mathcal{Z}$ within the cylinder (see figure 3). Although the *complete* exclusion of the negative l partial waves is quite sensitive to the proximity of the material to the zero index condition, in the supplementary material we show that the partial wave surface impedance Z_l remains highly sensitive to the sign of the incident angular momentum for a wide range of parameters around the zero index condition. We also show the effect of introducing a hole into the cylinder, demonstrating that this allows negative angular momenta waves to penetrate into the cylinder.

Highly degenerate bound states

The zero index condition (14) also affects bound states in electromagnetic materials, leading to highly degenerate bound states, where the number of degenerate states is determined

by an integral of an effective magnetic flux. Again, connecting with our discussion of the Dirac equation, the effect is identical to the degeneracy of the ground state ($E = \pm mc^2$) of a spin half particle in a magnetic field, where the degeneracy [25] is determined by the total magnetic flux, and more fundamentally by the Atiyah–Singer index theorem from differential geometry [26]. Further details of this analogy are given in the supplementary material.

FIG. 4. Bound states in a CAN medium with a pseudo magnetic field. An infinite cylinder (radius $R = 0.3\,\mathrm{m}$) of the material defined in equation (25), with parameters $\alpha = \beta = 1$, and a linear gradient in $\boldsymbol{a} = B(x\hat{\boldsymbol{x}} + y\hat{\boldsymbol{y}})$. The simulation is enclosed within a perfectly conducting $1\,\mathrm{m}^2$ box. The out of plane propagation constant is set at the fixed value $k_z = 25.13\,\mathrm{rad\,m^{-1}}$, indicated as the solid red line (a). (a) The 10 eigenvalues closest in magnitude to $k_0 = k_z$, calculated using COMSOL multiphysics [30], for increasing 'magnetic field' B. (b–e) Four of the degenerate eigenmodes at $B = 10$. Notice that in all four cases the modal phase advances anti–clockwise around the modal zeros, in accordance with analytic functions of $\mathcal{Z}$.

Consider modes that propagate out of the plane at fixed wave–vector $k_z = k$ (as we shall see in the next section, out of plane propagation mimics bianisotropy), and assume permittivity and permeability tensors of the form (translationally invariant along z)

$$\boldsymbol{\epsilon} = \frac{1}{\alpha}\begin{pmatrix} \mathbf{1}_2 & \mathrm{i}\boldsymbol{a}^{\mathrm{T}} \\ -\mathrm{i}\boldsymbol{a} & \beta \end{pmatrix} \qquad \boldsymbol{\mu} = \alpha\begin{pmatrix} \mathbf{1}_2 & \mathrm{i}\boldsymbol{a}^{\mathrm{T}} \\ -\mathrm{i}\boldsymbol{a} & \beta \end{pmatrix}. \tag{25}$$

where $\boldsymbol{a} = (a_x, a_y)$ is assumed to be graded in space. In the polarization basis $\Psi = E_z + \mathrm{i}\alpha\eta_0 H_z$ and $\boldsymbol{\Phi} = \boldsymbol{E}_\parallel + \mathrm{i}\alpha\eta_0\boldsymbol{H}_\parallel$, Maxwell's equations take the form $\boldsymbol{\nabla}\Psi \times \hat{\boldsymbol{z}} + \mathrm{i}k\hat{\boldsymbol{z}} \times \boldsymbol{\Phi} = k_0[\boldsymbol{\Phi} + \mathrm{i}\boldsymbol{a}\Psi]$, and $\boldsymbol{\nabla} \times \boldsymbol{\Phi} = k_0[\beta\Psi - \mathrm{i}\boldsymbol{a} \cdot \boldsymbol{\Phi}]\hat{\boldsymbol{z}}$. Comparison with the previous example in the case where $\boldsymbol{a} = 0$ we see that the limit $k \to k_0$ is equivalent to a zero index in the $\boldsymbol{m} = \hat{\boldsymbol{x}} - \mathrm{i}\hat{\boldsymbol{y}}$ direction, a result which will also be important in the next example.

We look for modes where the electromagnetic field is entirely in–plane, $\Psi = 0$, which requires

$$\begin{aligned} \left(\mathbf{1}_2 - \mathrm{i}\frac{k}{k_0}\hat{\boldsymbol{z}}\times\right) \cdot \boldsymbol{\Phi} &= 0 \\ \hat{\boldsymbol{z}} \cdot \boldsymbol{\nabla} \times \boldsymbol{\Phi} + \mathrm{i}k_0\boldsymbol{a} \cdot \boldsymbol{\Phi} &= 0 \end{aligned} \tag{26}$$

The first of (26) can be fulfilled in the zero index limit $k \to k_0$ if we write $\boldsymbol{\Phi} = (\hat{\boldsymbol{x}} + \mathrm{i}\hat{\boldsymbol{y}})\Phi$. Substituting this form of $\boldsymbol{\Phi}$ into (26) we find a first order differential equation for the scalar function Φ, $(\partial_x + \mathrm{i}\partial_y)\Phi + k_0(a_x + \mathrm{i}a_y)\Phi = 0$. Decomposing the vector $\boldsymbol{a}$ into transverse and longitudinal parts $\boldsymbol{a} = \boldsymbol{\nabla}\psi + \hat{\boldsymbol{z}} \times \boldsymbol{\nabla}\phi$, we have the following first order equation for the bound state amplitudes Φ

$$\left(\frac{\partial}{\partial x} + \mathrm{i}\frac{\partial}{\partial y}\right)\Phi + k_0\left(\frac{\partial \psi}{\partial x} + \mathrm{i}\frac{\partial \psi}{\partial y}\right)\Phi + \mathrm{i}k_0\left(\frac{\partial \phi}{\partial x} + \mathrm{i}\frac{\partial \phi}{\partial y}\right)\Phi = 0. \tag{27}$$

The general solution to (27) is

$$\Phi = f(x + \mathrm{i}y)\exp(-k_0\psi - \mathrm{i}k_0\phi), \tag{28}$$

where f is any analytic function of $\mathcal{Z} = x + \mathrm{i}y$. In an infinite medium (where the material parameter $\boldsymbol{a}$ would diverge at infinity), equation (28) shows that there are an infinite number of bound states at the frequency where $k = k_0$. In figure 4 we numerically calculate the 10 closest eigenfrequencies to that where this zero index condition is fulfilled, for increasing B. As B increases, the 10 modes shown are more tightly confined to the cylinder of material, eventually all becoming degenerate and fulfilling the zero index condition.

Unidirectional edge states

One of the remarkable predictions of topological photonics is that the difference in the bulk invariants (Chern numbers) of two materials can be used to predict the number and direction of states bound to their interface. Interfaces between CAN media can also support one–way interface states.

As an example, we again demand that the field $\Psi = E_z + \mathrm{i}\alpha\eta_0 H_z$ propagates with zero index, in the $\boldsymbol{m} = \hat{\boldsymbol{x}} + \mathrm{i}\hat{\boldsymbol{y}}$ direction. Expanding out equation (11), condition (12) is

$$\begin{aligned} \boldsymbol{m} \cdot \left(\boldsymbol{\epsilon} + \mathrm{i}\alpha^{-1}\boldsymbol{\xi}^\dagger\right) &= 0 \\ \boldsymbol{m} \cdot (\boldsymbol{\mu} - \mathrm{i}\alpha\boldsymbol{\xi}) &= 0 \end{aligned} \tag{29}$$

We make the following choice of material parameters, which is a factor of i different from (20)

$$\boldsymbol{\epsilon} = \alpha^{-1}\mathbf{1}_3,\ \boldsymbol{\mu} = \alpha\mathbf{1}_3,\ \boldsymbol{\xi} = \lambda\begin{pmatrix} 0 & 1 & 0 \\ -1 & 0 & 0 \\ 0 & 0 & 0 \end{pmatrix} = -\lambda\hat{\boldsymbol{z}}\times\,. \tag{30}$$

This material is equivalent to a medium moving with velocity $\boldsymbol{V} = -\lambda c\hat{\boldsymbol{z}}$ (see Silveirinha [21], for a discussion of scattering anomalies in moving media). In the limit $\lambda \to 1$ (luminal motion), Ψ becomes an analytic function of $\mathcal{Z} = x + \mathrm{i}y$. This analyticity leads to unidirectional interface states, and we now consider the problem of waves trapped at the interface of two media where $\lambda = \pm 1$ (i.e. two media that are the time reverse of one another). Specifically we vary the bianisotropy in space with $\lambda(x) = |\lambda| \operatorname{sign}(x)$.

FIG. 5. Unidirectional edge modes between a pair of time reversed CAN media, and similar unidirectional propagation evident in total internal reflection. (a–b) The bianisotropic media have the constitutive relations (30) with material parameters $\alpha = 1$ and indicated values of λ. Decomposing the field into the polarizations $E_z \pm \mathrm{i}H_z$, each is constrained to propagate in only one direction. See the supplementary material for the modifications to COMSOL Multiphysics [30] necessary to simulate bianisotropic materials. (c–d) Field (32) due to total internal reflection within a material with $\epsilon = 1.5$, $k_z = -k_0$, and $k_y = 0.2k_0$. In the two panels we resolve the field into the polarizations indicated, showing that only the field $E_z + \mathrm{i}\eta_0 H_z$ can propagate outside the dielectric when $k_y < 0$.

For the parameters (30) Maxwell's equations take the same form as in our previous example, with the substitutions $\boldsymbol{a} = 0$, $\beta = 1$, and $k = -k_0\lambda$. From the continuity of the in–plane $\boldsymbol{E}$ and $\boldsymbol{H}$ fields across the interface at $x = 0$, we have continuity of both Ψ and $\Phi_y = E_y + \mathrm{i}\alpha\eta_0 H_y$. Using Maxwell's equations to write Φ_y in terms of Ψ, and assuming propagation along the interface $\partial_y \to \mathrm{i}k_y$, we have

$$-\frac{\partial \Psi}{\partial x} + k_y|\lambda| \operatorname{sign}(x)\Psi \qquad \text{continuous at } x = 0 \tag{31}$$

In order that the mode be bound to the interface, it must have a $\exp(-\kappa|x|)$ dependence, with $\kappa > 0$. Equation (31) is therefore equivalent to the continuity of $\operatorname{sign}(x)(\kappa + k_y|\lambda|)$, which can only be fulfilled if $\kappa = -k_y|\lambda|$. The interface state is therefore unidirectional, only existing for negative k_y. As predicted, when $\lambda = +1$ the interface state becomes respectively an analytic function of $\mathcal{Z}^\star$, and $\mathcal{Z}$ on the two sides of the interface. Note that there is unidirectional propagation for any value of $|\lambda| > 1$. Panels (a) and (b) of figure 5 show a full wave simulation of a magnetic line source next to the interface between the two media (30). Decomposing the resulting field into the two polarizations $E_z \pm \mathrm{i}\eta_0 H_z$ shows that, as predicted each polarization is constrained to propagate in only direction along the interface.

Evanescent waves

The material parameters given in equation (30) are equivalent to luminal motion of a dielectric, which is difficult to experimentally investigate. Yet in the case where $\boldsymbol{\xi}$ is homogeneous in space, the material can be easily obtained. It is equivalent to an isotropic material with $\epsilon = 1/\mu$ (e.g. vacuum), through which a wave propagates with out of plane wave–vector $k_z = -\lambda k_0$ along the z–axis. As shown in our discussion of bound states, out of plane propagation mimics bianisotropy. This can be seen very simply through writing Maxwell's equations as e.g. $\boldsymbol{\nabla} E_z \times \hat{\boldsymbol{z}} + \mathrm{i}k_z \hat{\boldsymbol{z}} \times \boldsymbol{E}_{\parallel} = \mathrm{i}k_0 \eta_0 \mu \boldsymbol{H}_{\parallel}$. The term proportional to k_z appears as an effective bianisotropic response $\boldsymbol{\xi} = (k_z/k_0)\hat{\boldsymbol{z}}\times = -\lambda \hat{\boldsymbol{z}}\times$ (c.f. equation (30)). With this identification, we can assign an effective bianisotropy to any material, even free space. This identification can be understood as already present in previous work on topological insulators where out of plane propagation was used to break time reversal symmetry in discrete [27] and continuous [28] systems.

FIG. 6. The out of plane field E_z of a surface plasmon excited by a chiral antenna. The simulation was performed using COMSOL Multiphysics [30]. The chiral antenna excites only one of the polarizations $E_z \pm \mathrm{i}\eta_0 H_z$ and is modelled using an electric and magnetic line current aligned along the z–axis, positioned where the white dot is shown. The amplitude of the magnetic line current is equal to that of the electric current times the free space impedance, and the phase is different by either (a) $+\pi/2$, or (b) $-\pi/2$. Along the axis of the antenna the current has a propagation vector $k_z = -k_0$.

Using this equivalence between bianisotropy and out of plane propagation in free space, the above unidirectional edge state can be found in any evanescent wave. In this particular case of our zero index condition, the unidirectional propagation is equivalent to the spin–momentum locking of evanescent waves recently identified by Bliokh and coworkers [29].

The simplest case is total internal reflection. We have a semi–infinite dielectric medium in the region $x < 0$ with $\epsilon = n^2 > 1$. An E polarized wave is incident from inside the

medium onto the interface at $x = 0$. The out of plane fields are given by

$$E_z = \frac{E_0 k_y}{\sqrt{k_y^2 + k_z^2}} \mathrm{e}^{\mathrm{i}\boldsymbol{k}_\parallel \cdot \boldsymbol{x}} \begin{cases} \mathrm{e}^{\mathrm{i}k_x x} + r\mathrm{e}^{-\mathrm{i}k_x x} & x < 0 \\ t\mathrm{e}^{\mathrm{i}k'_x x} & x > 0 \end{cases}$$
$$\eta_0 H_z = \frac{E_0 \lambda}{\sqrt{k_y^2 + k_z^2}} \mathrm{e}^{\mathrm{i}\boldsymbol{k}_\parallel \cdot \boldsymbol{x}} \begin{cases} k_x(\mathrm{e}^{\mathrm{i}k_x x} - r\mathrm{e}^{-\mathrm{i}k_x x}) & x < 0 \\ k'_x t\mathrm{e}^{\mathrm{i}k'_x x} & x > 0 \end{cases} \tag{32}$$

where $k_x = \sqrt{(\epsilon - \lambda^2)k_0^2 - k_y^2}$ and $k'_x = \sqrt{(1 - \lambda^2)k_0^2 - k_y^2}$, and the reflection and transmission coefficients are $r = (k_x - k'_x)/(k_x + k'_x)$ and $t = 2k_x/(k_x + k'_x)$. Using equation (32) to calculate the combination of out of plane field components $\Psi = E_z + \mathrm{i}\eta_0 H_z$, in the limit $\lambda \to +1$ we find

$$\lim_{\lambda \to 1} \Psi = -\frac{2|k_y|t}{\sqrt{k_y^2 + k_z^2}} \begin{cases} 0 & k_y > 0 \\ \mathrm{e}^{-|k_y|(x + \mathrm{i}\, y)} & k_y < 0 \end{cases} \tag{33}$$

Therefore for total internal reflection where the internal propagation angle is such that $k_z = -k_0$, the field component Ψ outside the medium becomes an analytic function of $\mathcal{Z} = x + \mathrm{i}y$, as shown in panels (c) and (d) in figure 5. Here the wave is incident from inside the dielectric with $k_z = -k_0$ and $k_y = -0.2k_0$. Plotting the two polarizations $\Psi = E_z \pm \mathrm{i}\eta_0 H_z$, we see that only $E_z + \mathrm{i}\eta_0 H_z$ is non zero outside the dielectric. This is true for any evanescent wave, as pointed out in [29].

In figure 6 we show the out of plane electric field E_z obtained from a chiral source next to a metal with $\epsilon = -2$. The source is a chiral antenna extended along the z–axis, with propagation vector $k_z = -k_0$ along the axis of the antenna. The source is modelled using a combined electric current $j_z = J\mathrm{e}^{-\mathrm{i}k_0 z}$ and magnetic current $m_z = \pm\mathrm{i}\eta_0 J\mathrm{e}^{-\mathrm{i}k_0 z}$ at the point indicated with the white dot. Such a source excites only one of the polarizations $E_z \pm \mathrm{i}\eta_0 H_z$, which propagates in only one direction along the surface.

CONCLUDING REMARKS

Our concept of a circulation dependent refractive index connects the two dimensional Dirac equation, complex analysis, and crystal optics, and provides a new means to understand and design electromagnetic materials supporting one–way propagation. Not only does this provide an alternative viewpoint on many of the results in topological photonics, but it

also reveals that devices such as circulation dependent sources, and waveguides exhibiting a large mode degeneracy can be designed through considering the complex analytic properties of the electromagnetic wave. In this work we focussed on lossless media, where the material tensor is a Hermitian matrix, but it would be straightforward and interesting to consider the case of non-Hermitian media. Furthermore, analogous results to those given here presumably apply in acoustics, fluid dynamics, and elastodynamics, where many results derived using topology remain difficult to intuit.

ACKNOWLEDGMENTS

SARH acknowledges financial support from a Royal Society TATA University Research Fellowship (RPG-2016-186). MW acknowledges funding from an EPSRC vacation bursary. SARH acknowledges useful conversations with W. L. Barnes and I. R. Hooper, as well as I. R. Hooper's numerical expertise. Both authors acknowledge extremely helpful and constructive suggestions from the referees, which led to significant work that greatly improved the manuscript.

AUTHOR CONTRIBUTIONS

SARH devised the theory and wrote the manuscript. MW contributed to the theory, commented on the manuscript, and wrote the numerical code to produce Fig. 1.

COMPETING INTERESTS

SARH and MW declare no competing interests.

DATA AVAILABILITY

Source data are available for this paper. All other data that support the plots within this paper and other findings of this study are available from the corresponding author upon reasonable request.

CODE AVAILABILITY

Figures were generated using Mathematica and Python, and full wave simulations were performed using COMSOL Multiphysics 5.4. Mathematica and Python code and COMSOL models are available from the corresponding author upon reasonable request.

---

[1] A. Mark Smith. *From Sight to Light: The Passage from Ancient to Modern Optics*. University of Chicago Press, 2015.

[2] T. Young. *A Course of Lectures on Natural Philosophy and the Mechanical Arts, Volume 1*. Franklin Classics Trade Press, 2018.

[3] M. Kadic, G. W. Milton, M. van Hecke, and M. Wegener. 3D metamaterials. *Nat. Rev. Phys.*, 1:198–210, 2019.

[4] A. Guo, G. J. Salamo, D. Duchesne, R. Morandotti, M. Volatier-Ravat, V. Aimez, G. A. Siviloglou, and D. N. Christodoulides. Observation of $\mathcal{PT}$-symmetry breaking in complex optical potentials. *Phys. Rev. Lett.*, 103:093902, 2009.

[5] S. A. R. Horsley, M. Artoni, and G. C. La Rocca. Spatial Kramers-Kronig relations and the reflection of waves. *Nat. Phot.*, 9:436–439, 2015.

[6] J. B. Pendry. Negative Refraction Makes a Perfect Lens. *Phys. Rev. Lett.*, 85:3966–3969, 2000.

[7] M. Silveirinha and N. Engheta. Tunneling of Electromagnetic Energy through Subwavelength Channels and Bends. *Phys. Rev. Lett.*, 97:157403, 2006.

[8] U. Leonhardt and T. G. Philbin. *Geometry and Light: The Science of Invisibility*. Dover, 2010.

[9] B. Edwards, A. Alù, M. E. Young, M. G. Silveirinha, and N. Engheta. Experimental Verification of Epsilon-Near-Zero Metamaterial Coupling and Energy Squeezing Using a Microwave Waveguide. *Phys. Rev. Lett.*, 100:033903, 2008.

[10] I. Liberal, A. M. Mahmoud, Y. Li, B. Edwards, and N. Engheta. Photonic doping of epsilon-near-zero media. *Science*, 355:1058–1062, 2017.

[11] A. R. Davoyan and N. Engheta. Theory of wave propagation in magnetized near-zero-epsilon metamaterials: Evidence for one-way photonic states and magnetically switched transparency

and opacity. *Phys. Rev. Lett.*, 111:257401, 2013.

[12] M. G. Silveirinha. Chern invariants for continuous media. *Phys. Rev. B*, 92:125153, 2015.

[13] S. A. R. Horsley. Unidirectional wave propagation in media with complex principal axes. *Phys. Rev. A*, 97:023834, 2018.

[14] S. A. R. Horsley. Topology and the optical Dirac equation. *Phys. Rev. A*, 98:043837, 2018.

[15] B. Thaller. *The Dirac Equation*. Springer, 2013.

[16] M. Z. Hasan and C L Kane. Colloquium: Topological Insulators. *Rev. Mod. Phys.*, 82(4):3045–3067, 2010.

[17] S. M. Barnett. Optical Dirac equation. *New J. Phys.*, 16:093008, 2014.

[18] S. A. R. Horsley. Indifferent electromagnetic modes: bound states and topology. *Phys. Rev. A*, 100:053819, 2019.

[19] T. V. Mechelen and Z. Jacob. Photonic Dirac monopoles and skyrmions: spin-1 quantization. *Opt. Mater. Express*, 9:95–111, 2019.

[20] W. L. Barnes, S. A. R. Horsley, and W. L. Vos. Classical antennas, quantum emitters, and densities of optical states. *J. Opt.*, 22:073501, 2020.

[21] M. G. Silveirinha. $\mathcal{P} \cdot \mathcal{T} \cdot \mathcal{D}$ Symmetry Protected Scattering Anomaly in Optics. *Phys. Rev. B*, 95:035153, 2017.

[22] A. B. Khanikaev, S. H. Mousavi, T. Wang-Kong, M. Kargarian, A. H. MacDonald, and G. Shvets. Photonic topological insulators. *Nat. Mat.*, 12:233–239, 2013.

[23] Liu. F. and J. Li. Gauge Field Optics with Anisotropic Media. *Phys. Rev. Lett.*, 114:103902, 2015.

[24] F. W. J. Olver, A. B. Olde Daalhuis, D. W. Lozier, B. I. Schneider, R. F. Boisvert, C. W. Clark, B. R. Miller, and B. V. Saunders. NIST Digital Library of Mathematical Functions (Release 1.0.23 of 2019-06-15.). http://dlmf.nist.gov/.

[25] Y Aharonov and A Casher. Ground state of a spin-1/2 charged particle in a two-dimensional magnetic field. *Phys. Rev. A*, 19:2461–2462, 1978.

[26] M. F. Atiyah and I. M. Singer. The index of elliptic operators on compact manifolds. *Bull. Am. Math. Soc.*, 69:422–433, 1969.

[27] M. C. Rechtsman, J. M. Zeuner, Y. Plotnik, Y. Lumer, D. Podolsky, F. Dreisow, S. Nolte, M. Segev, and A. Szameit. Photonic floquet topological insulators. *Nature*, 496:196–200, 2013.

[28] W. Gao, M. Lawrence, B. Yang, F. Liu, F. Fang, B. Beri, J. Li, and S. Zhang. Topological photonic phase in chiral hyperbolic metamaterials. *Phys. Rev. Lett.*, 114:037402, 2015.

[29] K. Y. Bliokh, D. Smirnova, and F. Nori. Quantum spin Hall effect of light. *Science*, 348:1448–1451, 2015.

[30] COMSOL Multiphysics ® v. 4.4. http://www.comsol.com.

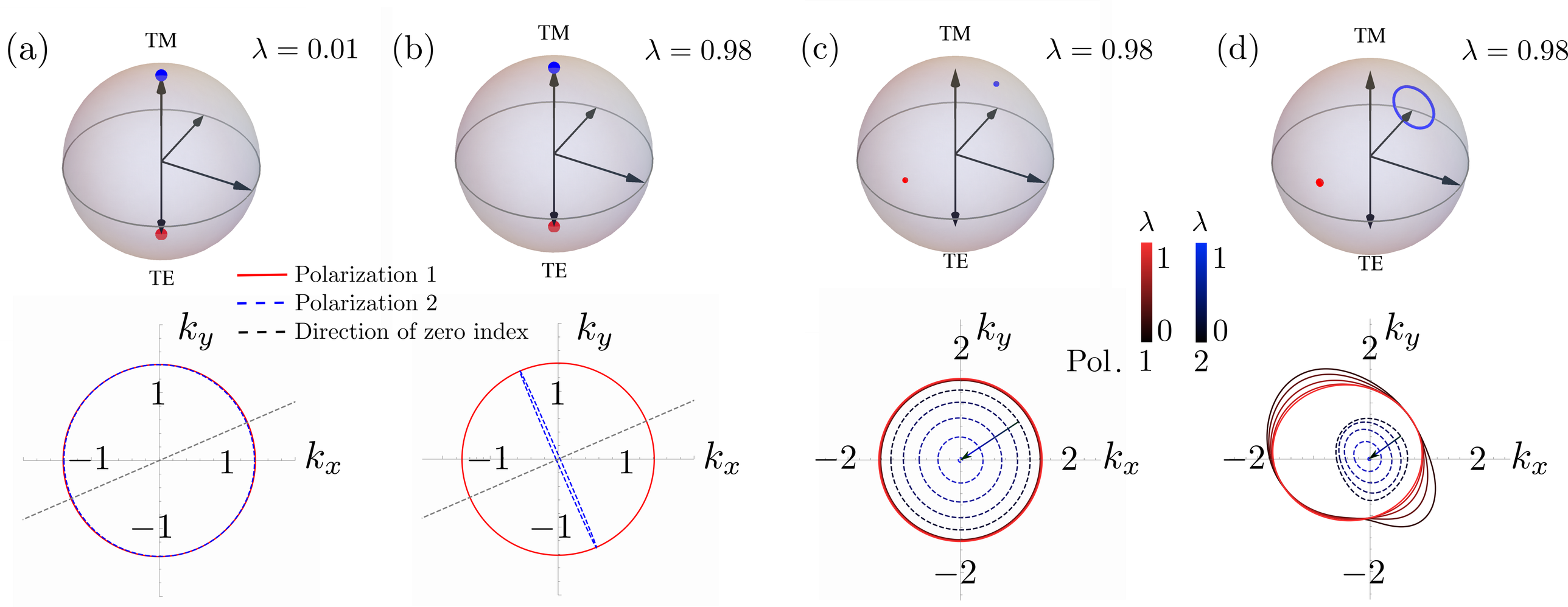
(a)
TM
$\lambda = 0.01$
TE
(b)
TM
$\lambda = 0.98$
TE
(c)
TM
$\lambda = 0.98$
TE
(d)
TM
$\lambda = 0.98$
TE
Polarization 1
Polarization 2
Direction of zero index
k_y
k_x
1
−1
λ
1
0
Pol. 1
λ
1
0
2
−2

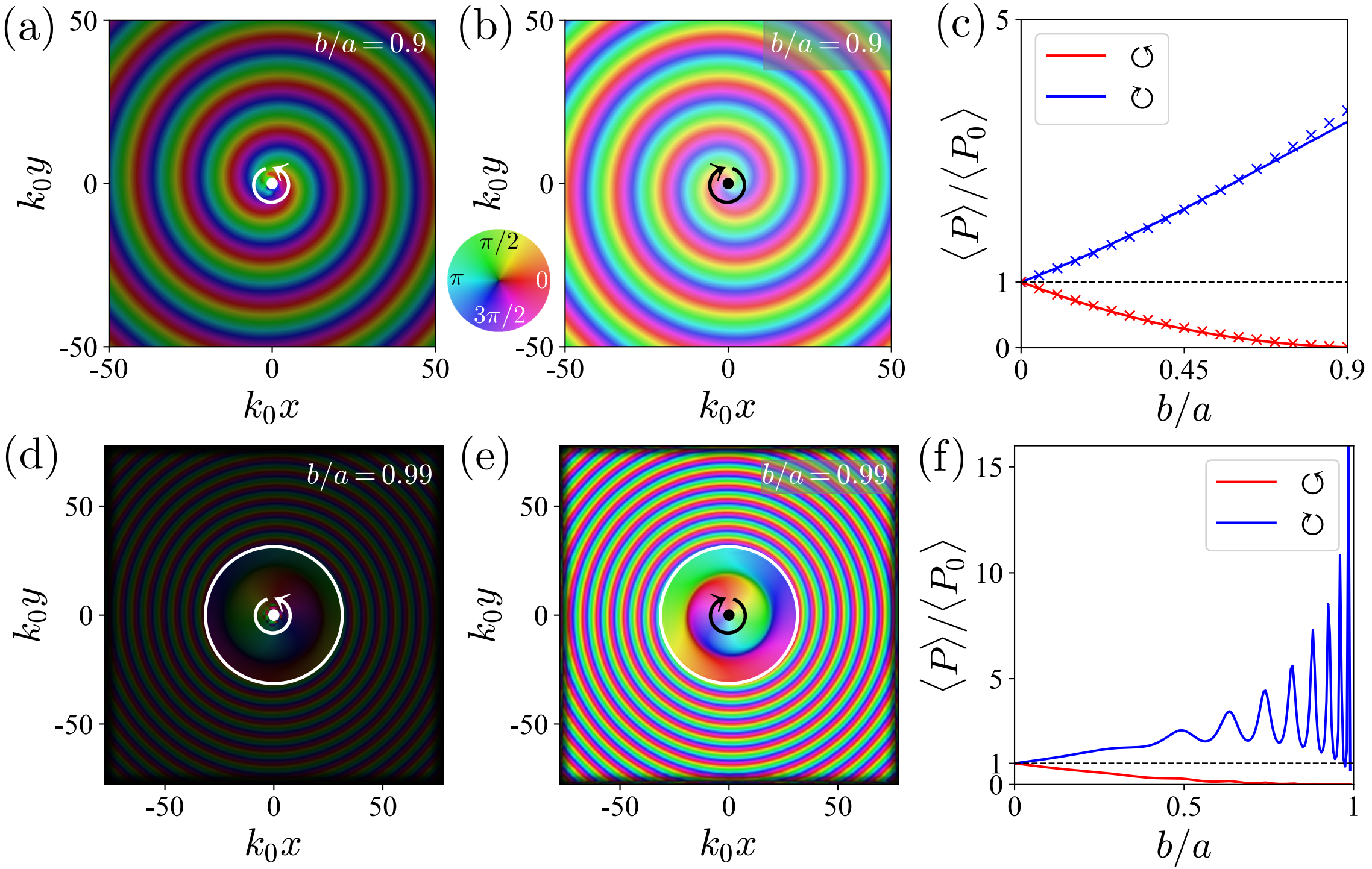
(a)
$b/a = 0.9$
$k_0 y$
$k_0 x$
50
0
-50
(b)
$b/a = 0.9$
$\pi/2$
π
0
$3\pi/2$
(c)
$\langle P \rangle / \langle P_0 \rangle$
0.45
0.9
b/a
5
1
(d)
$b/a = 0.99$
(e)
$b/a = 0.99$
(f)
15
10
0.5
1

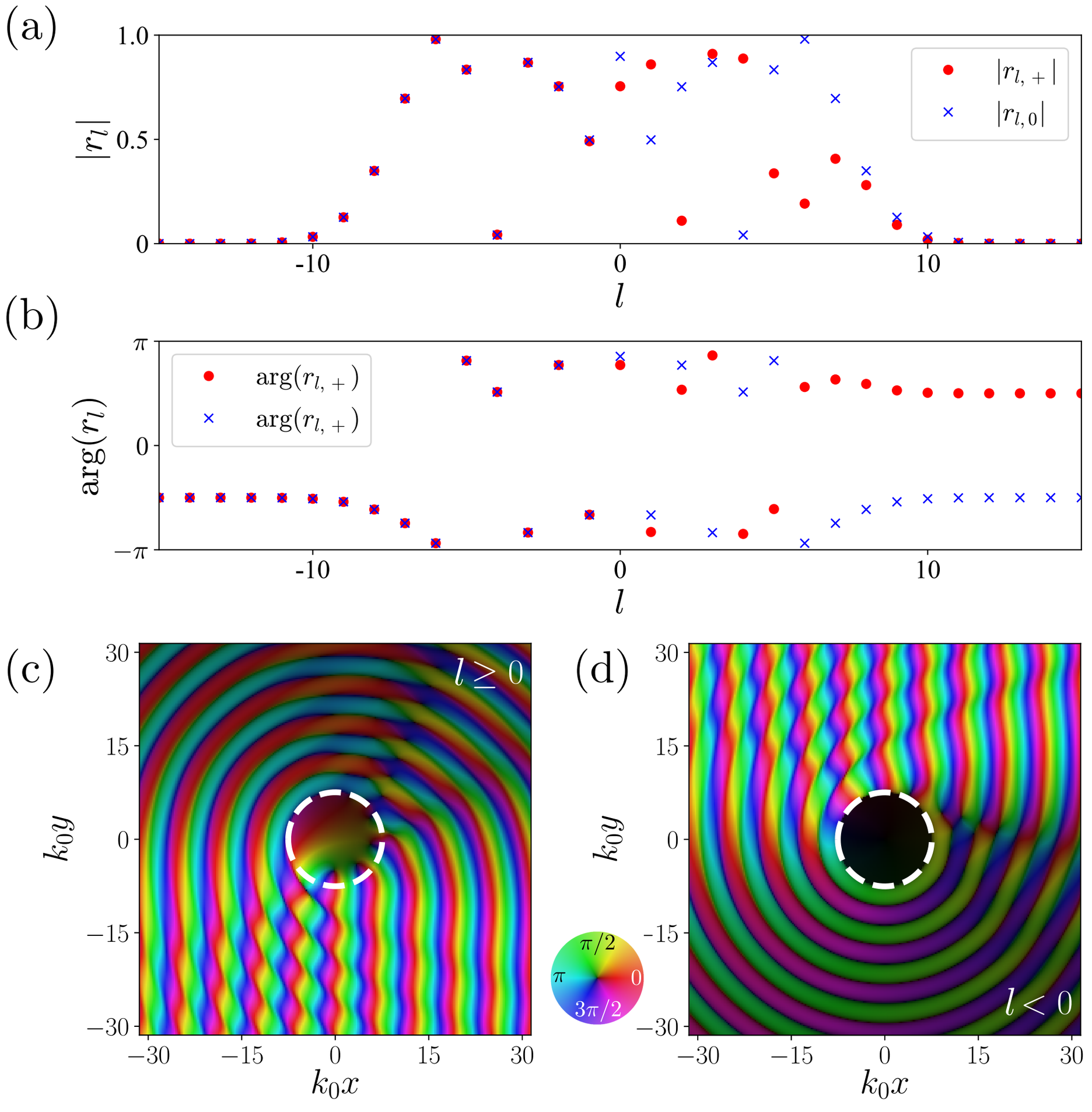
(a)
1.0
0.5
0
$|r_l|$
-10
0
10
l
$|r_{l,+}|$
$|r_{l,0}|$
(b)
π
0
$-\pi$
$\arg(r_l)$
-10
0
10
l
$\arg(r_{l,+})$
$\arg(r_{l,+})$
(c)
$l \geq 0$
30
15
0
−15
−30
k_0y
−30
−15
0
15
30
k_0x
(d)
$l < 0$
$\pi/2$
π
0
$3\pi/2$

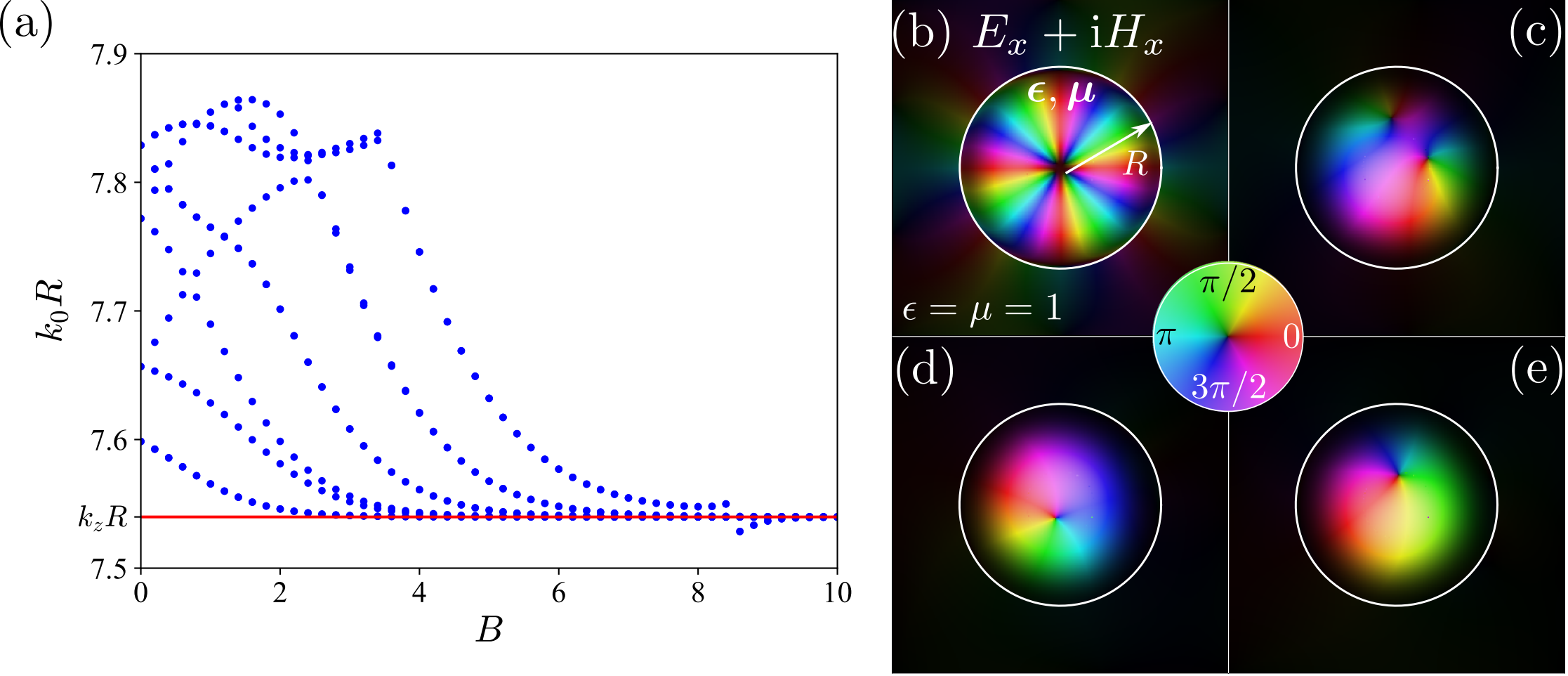
(a)
7.9
7.8
7.7
7.6
7.5
k_0R
k_zR
0
2
4
6
8
10
B
(b) $E_x + \mathrm{i}H_x$
ϵ, μ
R
$\epsilon = \mu = 1$
(c)
$\pi/2$
π
0
$3\pi/2$
(d)
(e)

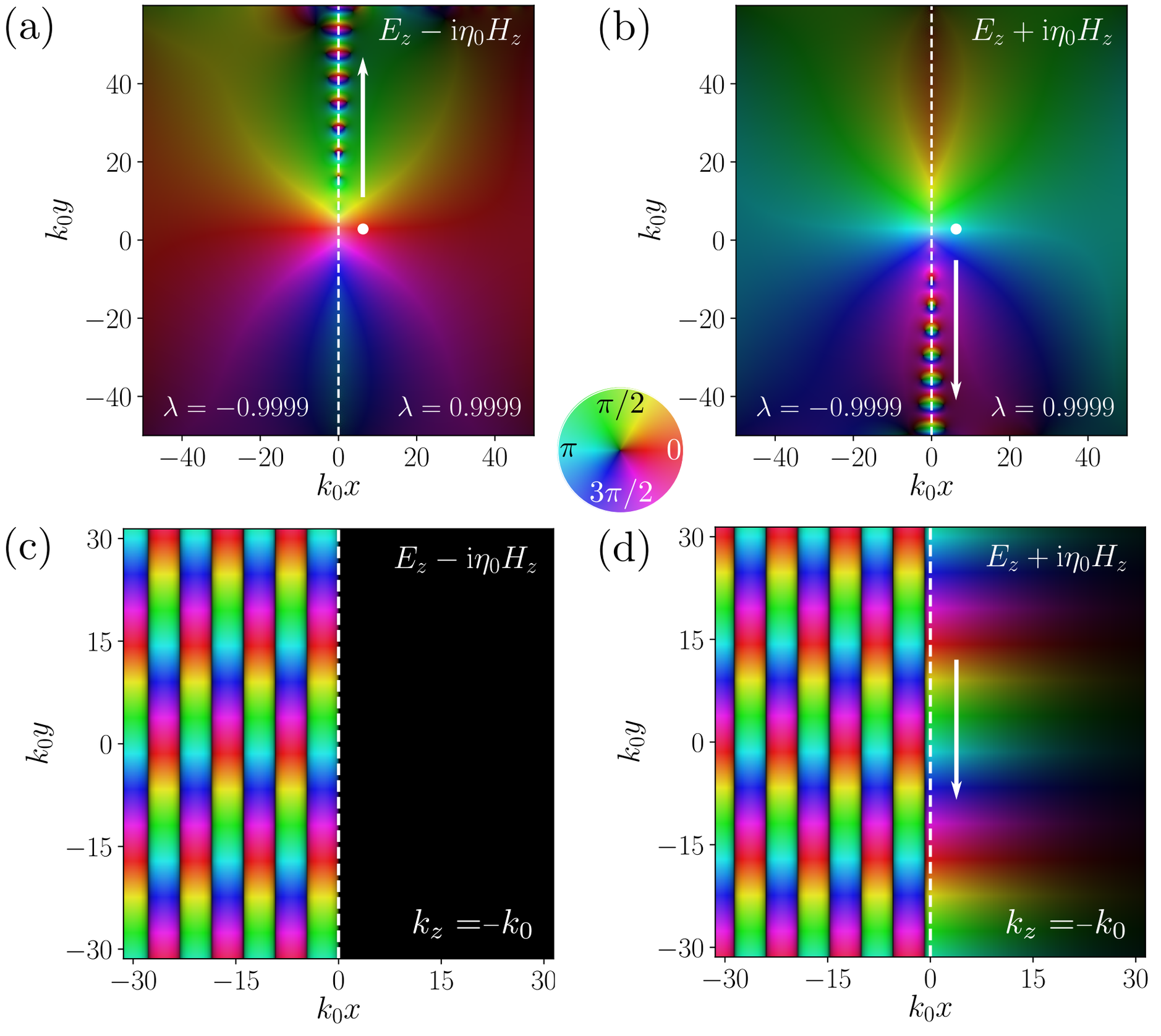
(a)
$E_z - \mathrm{i}\eta_0 H_z$
$\lambda = -0.9999$
$\lambda = 0.9999$
$k_0 y$
$k_0 x$
(b)
$E_z + \mathrm{i}\eta_0 H_z$
$\lambda = -0.9999$
$\lambda = 0.9999$
$k_0 y$
$k_0 x$
$\pi/2$
π
0
$3\pi/2$
(c)
$E_z - \mathrm{i}\eta_0 H_z$
$k_z = -k_0$
$k_0 y$
$k_0 x$
(d)
$E_z + \mathrm{i}\eta_0 H_z$
$k_z = -k_0$
$k_0 y$
$k_0 x$

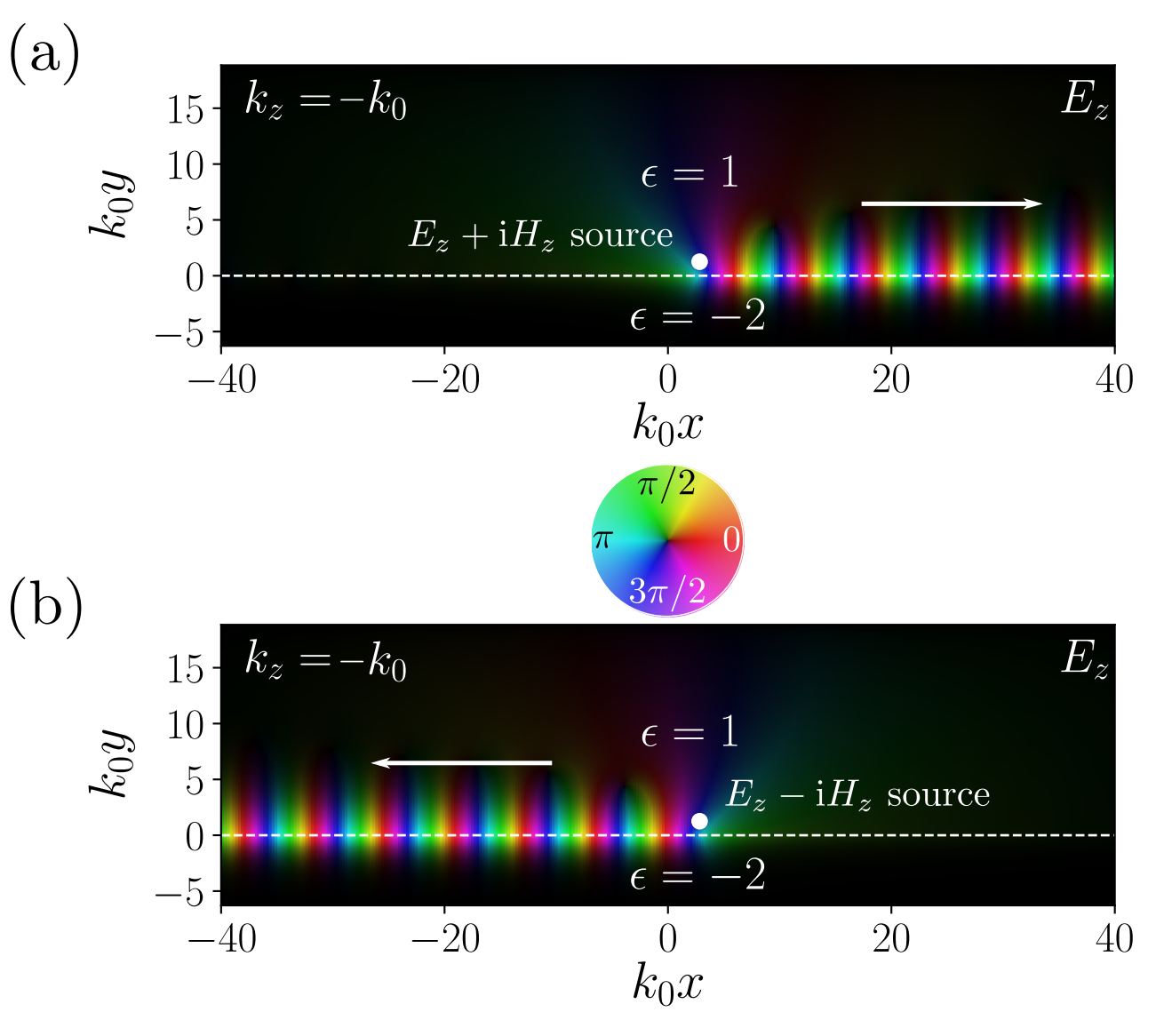
(a)
$k_z = -k_0$
E_z
$\epsilon = 1$
$E_z + \mathrm{i}H_z$ source
$\epsilon = -2$
15
10
5
0
−5
$k_0 y$
−40
−20
0
20
40
$k_0 x$
π/2
π
0
3π/2
(b)
$k_z = -k_0$
E_z
$\epsilon = 1$
$E_z - \mathrm{i}H_z$ source
$\epsilon = -2$
15
10
5
0
−5
$k_0 y$
−40
−20
0
20
40
$k_0 x$